



Published in final edited form as:

Clin Cancer Res. 2020 June 15; 26(12): 2898–2907. doi:10.1158/1078-0432.CCR-19-1272.

A quantitative centrosomal amplification score predicts local recurrence of ductal carcinoma in situ

Karuna Mittal¹, Michael S. Toss^{2, #}, Guanhao Wei^{1, #}, Jaspreet Kaur^{1, #}, Da Hoon Choi¹, Brian D. Melton¹, Remus M. Osan¹, Islam M. Miligy², Andrew R Green², Emiel A. M. Janssen³, Håvard Søliland⁴, Keerthi Gogineni⁵, Upender Manne⁶, Padmashree Rida^{1, 7, *}, Emad A. Rakha^{2, *}, Ritu Aneja^{1, *}

¹Department of Biology, Georgia State University, Atlanta, GA, USA

²University of Nottingham and Nottingham University Hospitals Nottingham, UK

³Department of Pathology, Stavanger University Hospital, Stavanger, Norway

⁴Department of Breast and Endocrine Surgery, Stavanger University Hospital, Stavanger, Norway

⁵Emory University School of Medicine; Atlanta, GA, USA

⁶Department of Pathology, University of Alabama School of Medicine, AL, USA;

⁷Novazoi Theranostics, Inc., Rolling Hills Estates, CA, USA

Abstract

Purpose: To predict risk of local recurrence (LR) in ductal carcinoma in situ (DCIS) with a new visualization and quantification approach using centrosome amplification (CA), a cancer-cell specific trait, widely associated with aggressiveness.

Experimental Design: This first-of-its-kind methodology evaluates the severity and frequency of numerical and structural CA present within DCIS, and assigns a quantitative centrosomal amplification score (CAS) to each sample. Analyses were performed in a discovery cohort (DC, n=133) and a validation cohort (VC, n=119).

Results: DCIS cases with LR exhibited significantly higher CAS than recurrence-free cases. Higher CAS was associated with a greater risk of developing LR (HR=6.3 and 4.8 for DC and VC, respectively; p<0.001). CAS remained an independent predictor of relapse-free survival (HR=7.4 and 4.5 for DC and VC, respectively; p<0.001) even after accounting for potentially confounding factors (grade, age, comedo necrosis and radiotherapy). Patient stratification using CAS (p<0.0001) was superior to that by Van Nuys Prognostic Index (VNPI) (HR for CAS=6.2, vs. HR for VNPI=1.1). Among patients treated with breast-conserving surgery alone, CAS identified patients likely to benefit from adjuvant radiotherapy (RT).

*Corresponding authors: Ritu Aneja, Department of Biology, Georgia State University, 100 Piedmont Ave, Atlanta GA 30303, Office: 404-413-5417 Fax: 404-413-5301, raneja@gsu.edu, Emad A. Rakha, Division of Cancer and Stem Cells, School of Medicine, University of Nottingham City Hospital Campus, Hucknall Road, Nottingham, NG5 1PB, UK, Telephone: 01159691169 Ext: 56416, Fax: (+44) 01159627768, Emad.Rakha@nottingham.ac.uk, Emad.Rakha@nuh.nhs.uk, Padmashree Rida, Novazoi Theranostics, Inc., Rolling Hills Estates, CA, USA, cgp_rida@yahoo.com.

#Contributed equally to the study

Competing interests: The authors declare no competing financial interests.

Conclusions: CAS predicted 10-year LR risk for patients who underwent surgical management alone and identified patients who may be at low risk of recurrence, and for whom adjuvant RT may not be required. CAS demonstrated the highest concordance among the known prognostic models such as VNPI and clinicopathological variables such as grade, age, and comedo necrosis.

Translational Relevance: This is the first study to quantitate amplified centrosomes using a semi-automated pipeline technology that integrates immunofluorescence confocal microscopy with digital image analysis to generate a quantitative centrosome amplification score (CAS). CAS is a summation of the severity and frequency of centrosomal aberrations in clinical tumor samples. Our study represents the first step in developing CAS as a readily quantifiable biomarker that can predict the risk of local recurrence (LR) in DCIS with higher concordance than existing predictive tools. CAS stratifies lumpectomy cases into “low-CA DCIS” and “high-CA DCIS” wherein “high-CA DCIS” are much more likely to have LR, thereby aiding treatment decision-making. This study is also the first to highlight organellar-level differences between recurrent and non-recurrent DCIS. CAS may serve as a promising new clinical tool to aid decision-making and improve treatment recommendations for DCIS patients.

INTRODUCTION

Approximately 20% of screen-detected breast cancers (BC) are DCIS, a pre-invasive form of BC wherein malignant epithelial cells are confined to the lumen of a mammary duct and do not invade into the adjacent stroma (1,2). Notably, 20–53% of women with untreated DCIS progress to invasive BC over a period of 10 years (3). Since the progressive potential of a DCIS lesion cannot be reliably determined, local control via surgical excision with or without local radiotherapy is the mainstay strategy, with addition of endocrine blockade in some cases (4). Unfortunately, 10–35% of DCIS patients treated with lumpectomy or breast conservation surgery (BCS) later present with a local recurrence (LR) and about half of all recurrences occur in the form of invasive breast cancer (IBC) (5,6). A major challenge is to avoid under- or over-treatment by developing prognostic biomarkers that can stratify DCIS patients based on their recurrence risk.

Current predictors of recurrence risk for DCIS such as the Van Nuys Prognostic Index (VNPI) (7) and the Memorial Sloan Kettering DCIS nomogram (8) are based on routinely-used clinicopathological parameters but lack consistency and reproducibility in risk prediction (9,10). In addition, these tools do not integrate prognostically-informative molecular predictors, and underestimate DCIS heterogeneity. While Oncotype Dx Breast DCIS score, a commercially-available gene-expression based assay, has some value in predicting LR, it has only been validated in two cohorts (ECOG E5194 and Ontario DCIS). The poor stratification of high/intermediate-risk patients in these two cohorts has called into question the prognostic value of this tool (11).

Extensive genetic and phenotypic intratumoral heterogeneity (ITH) characterizes DCIS (12,13). In a pre-invasive lesion, higher ITH predicts greater likelihood of LR and invasive BC (14). Amplified centrosomes underlie erroneous mitoses and fuel chromosomal instability (CIN), which is a well-recognized driver of ITH (15,16). Although normal cells have one centrosome pre- S-phase and two centrosomes post- S-phase, cancer cells

invariably display centrosome amplification (CA); an abnormal increase in the number (i.e., numerical amplification) and/or volume (i.e., structural amplification) of centrosomes (17). Semi-quantitative studies have shown that CA correlates with higher tumor grade, larger tumor size, disease recurrence and/or distant metastasis in various malignancies (18). Moreover, CA occurs within precancerous and preinvasive lesions including DCIS, suggesting that CA is an early event in tumorigenesis (19,20). CA increases with higher DCIS grade, and high-grade (HG) DCIS has elevated expression of Aurora-A and Nek2 kinases that are strongly associated with CA. In addition, the risk of LR in DCIS is predictable by dysregulation of genes like cyclin-D, cyclin-E, and p53/p21 that regulate the centrosome duplication process (21). In the present study, we postulated that recurrent and non-recurrent DCIS cases might differ in the extent and/or type of CA. The prognostic value of CA has remained unexplored for clinical application, as there is no methodology available for the rigorous quantitation of CA phenotypes. Also, it is unclear whether the prognostic value of CA lies in numerical and/or structural CA. It is unknown which of the two features of CA--frequency (i.e., percentage of cells showing amplified centrosomes), and/or severity (i.e., how abnormal the number/volume of centrosomes is in a given sample) --is prognostically informative.

Herein, we present a new methodology for centrosomal phenotyping to quantitate both numerical and structural centrosomal aberrations in clinical tissue samples. Centrosomes were immunofluorescently stained using an antibody against γ -tubulin, and co-stained nuclei with Hoechst. Our analytical procedure allows robust interrogation of the capacity of centrosomal overload to predict the risk of LR after a lumpectomy. We have developed an algorithm that quantitates the frequency/prevalence and severity of CA (both numerical and structural) in formalin-fixed paraffin-embedded (FFPE) clinical samples, and computes a centrosome amplification score (CAS) for each sample. CAS is a promising metric that may improve treatment recommendations and allow identification of patients at low risk of recurrence for whom adjuvant RT may not be required. CAS demonstrates the highest concordance among the known prognostic models such as VNPI and commonly used clinicopathological variables such as grade, age, and comedo necrosis.

Materials and Methods

Clinical tissue samples

This is a retrospective study included FFPE tissue sections of primary pure DCIS consecutively diagnosed between 1988 and 2012 were obtained from Nottingham City Hospital, UK. Tumor tissue were preserved by standard approved processing methods using formalin fixation and embedding in paraffin. These tumor blocks were stored in the Nottingham tissue bank. Patients had (a) adequate amount of tissue, (b) available all relevant clinicopathologic data, and (c) at least 10 years of follow-up were eventually included in the study. The samples for the study were shared in three batches. For the pilot study to estimate the sample size, samples for the first 50 consecutive cases that met inclusion criteria were shared and based upon our findings, the proposed sample size of 116 for each cohort was expected to yield a power of 80% with an alpha of 0.05 (Supplementary Fig. 1). Subsequently, samples for the next 83 cases were shared which together with the earlier 50

samples formed the discovery cohort (DC). The validation cohort (VC) was received only after the study (staining, imaging, and image analysis) on the DC was completed. To exclude any bias, the GSU research group were totally blinded to clinicopathologic and outcome details of the patients included in the study. These data were not shared with GSU research team who performed the staining, imaging, and image analysis until the CAS scores were generated for each patient in all cohorts. The discovery cohort (DC) (n=133) and validation cohort (VC) (N=119) comprised of consecutive pure DCIS patients (no evidence of microinvasive or invasive breast cancer) with available tissue samples that showed free surgical margins >2mm (to avoid the effect of this confounder on the study outcome) and underwent BCS or mastectomy with or without adjuvant radiotherapy (RT) (Supplementary Fig. 2) (22–24). All cases were histologically reviewed, and diagnoses were confirmed by two independent pathologists (MST and IM, and in case of disagreement between the two reviewing pathologists the specialist breast pathologist (EAR) confirmed the diagnosis). All cases included data pertaining to their clinicopathologic variables such as age at diagnosis, menopausal status, DCIS size, nuclear grade, presence of comedo-type necrosis, treatment, VNPI, Ki67 proliferation index, and information about treatment (adjuvant RT), recurrence-free survival (RFS) defined by the time (in months) between 6 months after the first surgery and occurrence of ipsilateral LR in the form of either DCIS or IBC, date of initial diagnosis, date of surgery, and patient status at last contact (23). Patients who underwent completion surgery within the first 6 months after primary resection surgery due to positive/close surgical margins or presence of residual tumor tissue were not considered to have disease recurrence. All patients who developed contralateral breast events were censored at the time of development of the contralateral tumor. None of the patients in our discovery/validation cohorts received adjuvant endocrine therapy.

To determine normal volumes of the centrosomes, full-face sections of normal breast tissue from reduction mammoplasties (n=40) and breast tumors with extensive regions of adjacent uninvolved tissues (n=40) were obtained from Stavanger University Hospital, Norway, Nottingham City Hospital, UK, and West Georgia Hospital, GA, USA. All aspects of study were (a) approved by every Institutional Review Board, and (b) in compliance with guidelines in material transfer and data use agreements for all involved institutions, and Georgia State University (c) conducted in accordance with International Ethical Guidelines for Biomedical Research Involving Human Subjects. Informed consent was obtained from all subjects.

Immunofluorescence staining and confocal microscopy imaging of clinical samples

Centrosomes were immunofluorescently stained for γ -tubulin (red) and nuclei (with Hoechst) in paraffin-embedded sections of DCIS. Images of tissue samples were acquired with a Zeiss LSM 700 confocal microscope (using 63 \times oil immersion lens with a numerical aperture of 1.4 at 1.5 \times optical zoom). All imaging parameters were fixed across all samples. For optimal results, laser power was adjusted to the minimum level wherein fluorophore emission was saturated. For detector saturation, the gain (master) was adjusted such that the detector registers the target fluorophores in each channel within full range of detector settings (8-bit, 12-bit, 16-bit) to prevent over- and under-saturation and maximize accuracy. The offset was adjusted to minimize the background in the sample. Normal, DCIS and IBC

areas pre-marked by a pathologist were imaged to obtain at least 10 regions of interest (ROIs) each containing 20–30 nuclei and associated centrosomes (Fig. 1).

Scoring of centrosomes in clinical samples

Raw 3D image data were processed using IMARIS Biplane 8.2 3D volume rendering software to determine the volume of each centrosome within each ROI. “Volume rendering” refers to transforming a 2D image stack for 3D visualization and subsequent analysis. To exclude non-specific signals, a common background subtraction was applied to all images. This parameter was derived by first measuring the average diameter of ~100 centrosomes in 10 ROIs (Fig. 1), and then using the background corresponding to this average diameter as the background subtraction threshold. Finally, data from all optical sections were ordered to enable volume measurement for each centrosome. The final data of volumes of all centrosomes were then compared to a maximum intensity projection image and centrosomes for each cell were quantified based on proximity to their associated nuclei. The number and volume of all centrosomes associated with each nucleus in the tumor area were recorded.

Categorization of centrosomes into iCTRs and mCTRs

Centrosomes in breast tissue (normal, DCIS or IBC) were categorized into individually distinguishable centrosomes (iCTRs) and megacentrosomes (mCTRs). iCTRs were defined as centrosomes that stain positive for γ -tubulin; iCTR numbers and boundaries were clearly distinguishable, and their volumes lay within the range of centrosome volumes found in normal breast tissue stained for γ -tubulin. The volume range for a normal centrosome was determined by analyzing volumes of centrosomes from both adjacent uninvolved tissue from cancer patients and normal breast tissue from disease-free individuals (Supplementary Fig. 3). For adjacent uninvolved tissues, the selected cohort (n=40 patients) had a median age of 53.5 years (age range: 38–69.5 years). We evaluated centrosomal volumes in these samples as described in the analysis section. The mean centrosome volume for the adjacent uninvolved tissue sections was higher relative to the normal tissue from reduction mammoplasty. Thus, we chose the smallest and largest values for individual centrosome volume from normal tissue as the “normal centrosome volume range” for breast tissue. The mean volume of centrosomes in normal breast epithelial cells ranged from 0.2–0.74 μm^3 . Centrosomes with volumes $> 0.74 \mu\text{m}^3$ were categorized as mCTRs. All centrosomes in each ROI were thus categorized as iCTRs or mCTRs. In other words, mCTRs are centrosomes with aberrantly large volumes and are considered to represent structurally amplified centrosomes. The numbers and volumes of each iCTR and mCTR associated with each nucleus in an ROI were recorded.

Algorithm-based analytics

For each sample, a cumulative CAS (CAS_{total}) was computed based on the formula: CAS_{total} = CAS_i + CAS_m, where CAS_i and CAS_m are scores that describe numerical and structural CA phenotypes, respectively. Details on quantitation of numerical and structural CA are added in Supplementary data.

Statistical Analysis

Statistical analysis was accomplished with SAS 9.4 software (Cary, NC, USA), and the R-project version 3.4.3 (R Foundation for Statistical Computing, Vienna, Austria, <https://www.R-project.org/>). Raw CA volume data were converted to CASi, CASm and CASTotal according to the algorithm. Scaling factors recommended were used to normalize score of CASi and CASm in the range 0–3. Chi-square tests were performed to check recurrence proportions in patient subgroups. The tests of group mean differences shown in Box Plots were based on nonparametric Wilcoxon Rank Sum Tests and Kruskal-Wallis tests depending on the number of groups used for comparison, where the y-axis reflects the ranks of observations. RFS was used as the endpoint for the survival analysis (restricted to 10 years). The optimal cutoff (threshold used to categorize patients into high-or low-risk of LR subgroups) of the CASTotal value was selected based on the results of 133 log-rank tests. We simply set each possible CASTotal value from 133 cases in the DC as cutoff and then constructed Kaplan-Meier survival estimators for cases classified into high-risk and low-risk groups. The value 1.436 was finalized since it minimized the log-rank p-value. The same CASTotal cutoff was then used for the 119 cases from the VC to validate the model's effectiveness. Both univariate and multivariable Cox proportional hazard models, with age, grade, comedo necrosis, and RT controlled, were built to estimate Hazard Ratios (HRs) and 95% confidence intervals (CIs) between high vs. low CASTotal groups. A non-zero slope was detected in a generalized linear regression of the scaled Schoenfeld residuals on functions of time, which satisfied of the proportional hazards assumption (Supplementary Fig. 5). A 2×2 confusion matrix and performance metrics was used for sensitivity analysis. The fitted Cox models were also used to predict the approximate 10-year recurrence rate using SAS PROC PHREG module. For all tests p<0.05 was considered to be statistically significant.

Results:

Traditional clinicopathological variables have limited capacity to predict recurrence for DCIS patients

We found that among the 133 patients in the DC (details in Table 1), 28 patients developed ipsilateral LR. The median age at diagnosis was 58 years (age range: 41–84), and median follow-up was 132 months (14–333 months). Out of 133 patients, ~42% (n=55) received RT. Higher nuclear grade, the presence of comedo necrosis and the use of RT were clinicopathological parameters that showed proportional differences between recurring and LR-free patient subgroups (Table 1A). However, only high grade and comedo necrosis showed associations with RFS in a univariable Cox regression analysis (Table 2A). Intriguingly, none of these clinicopathological variables showed any significant association with RFS in multivariate analyses (Table 2A), thereby indicating the limited capacity of traditional clinicopathological variables to predict LR for DCIS in our DC. Our VC was also from Nottingham University Hospital, UK (patient characteristics in Table 1B) and comprised of 119 DCIS patients out of which 24 patients presented with ipsilateral LR. Median age of these patients was 56 years, and the median follow-up was 121 months. Histograms representing distribution of age and tumor size are added in the supplementary data (Supplementary Fig. 6). In addition we performed the KM survival analysis to show the

effect of standard prognostic markers like age, tumor size, radiotherapy and comedo necrosis on recurrence for the whole dataset (DC and VC, n=252) (Supplementary Fig. 7). Out of 119 patients, ~12% (n=14) received RT. In the VC, tumor size, presence of the comedo necrosis, and age, showed significant proportional differences between the LR and LR-free subgroups.

Recurrent DCIS patients show higher CAS compared to non-recurrent DCIS ones

Centrosome numbers and volumes, evaluated and scored for numerical (CASi) and structural (CASm) centrosomal aberrations (as described in methods) were integrated using our algorithm to generate a composite CASTotal value for each sample of the DC (Fig 2A, B). Interestingly, DCIS patients that developed LR within 10 years showed significantly higher CASi relative to LR-free patients ($p < 0.0001$; Fig. 2C). These patients with LR showed greater severity (CASi severity) ($p = 0.25$; Supplementary Fig. 8A) and higher frequency (CASi frequency) ($p < 0.0001$; Supplementary Fig. 8B) of numerical CA compared to LR-free patients. Analysis of structural CA revealed that CASm was significantly higher ($p = 0.04$, Fig. 2D) for the LR subgroup relative to LR-free subgroup. DCIS with LR exhibited greater severity (CASm severity) ($p = 0.01$, Supplementary Fig. 8C) and frequency (CASm frequency) ($p = 0.08$, Supplementary Fig. 8D) of structural CA compared to LR-free DCIS. Cumulatively, a summation of CASi and CASm generated CASTotal, which was significantly higher for DCIS patients with LR relative to LR-free patients regardless of grade (mean scores in Supplementary Table 1) (Fig. 2E).

Employing the same methodology for the VC, we calculated CAS (Supplementary Fig. 9) and found that irrespective of grade, DCIS cases with LR exhibited higher CASTotal relative to LR-free patients ($p < 0.0001$) (Fig. 2F). Further, similar trends were seen for other CAS subcomponents as observed in the DC; the ranked mean values of CASi ($p < 0.0001$) (Fig. 2G) and CASm ($p < 0.0001$) (Fig. 2H), including their severity (CASi severity $p = 0.0014$; CASm severity $p = 0.014$) and frequency (CASi frequency $p < 0.0001$, CASm frequency $p < 0.0001$) components, were higher in the patient subgroup with LR than in the LR-free subgroup (Supplementary Fig. 8 E, F,G,H).

Similar findings were evident for grade-matched patients in DC and VC (Supplementary Fig. 10) and patients that were treated only with BCS (Supplementary Fig. 11). Collectively, our data strongly suggest a stark difference in centrosomal aberrations between DCIS tumors of patients with and without LR.

Next, we co-immunolabeled 15 high-grade DCIS samples for both centrosomes (using anti γ -tubulin antibody) and centrioles (using anti-centrin-2 antibody) and generated CASTotal as described before. In all samples, γ -tubulin foci invariably overlapped with centrin-2 foci, confirming that both structurally and numerically amplified centrosomes are bona fide centrosomes and not simply aggregates of pericentriolar material. We also observed that none of the mCTRs had >2 centrin-2 foci, suggesting that enlarged γ -tubulin foci represent structurally augmented centrosomes and not supernumerary centrosomes that are tightly clustered to be indistinguishable (Supplementary Fig. 12).

CAS stratifies DCIS patients into subgroups with high- and low- risk of LR within 10 years of diagnosis

Upon stratification of all DC patients into low- and high-CAS groups (the threshold used was the one that minimized log-rank p-value) (Fig. 3), we found that DCIS patients with high CAS_i were associated with poorer RFS ($p < 0.001$, HR=4.80) relative to those with low CAS_i (Fig. 3A, Supplementary Fig. 13A, B, and Supplementary Table 2). Similarly, high CAS_m was associated with poorer RFS ($p = 0.04$, HR=2.396) compared to low CAS_m (Fig. 3B, Supplementary Fig. 13C, 13D, and Supplementary Table 2). CAS_{total} stratified the high-risk and low-risk DCIS patients with high significance and hazard ratio ($p < 0.001$, HR=6.3) (Fig. 3C). We found that 85.7% of patients with LR were in the high CAS_{total} group. This association with CAS_{total} remained significant ($p < 0.001$, HR=7.4) even after accounting for potential confounders, including comedo necrosis, tumor grade, age, RT, and receptor status (Table 2A). Although presence of comedo necrosis and CAS_{total} were associated with RFS in univariate analyses, only CAS_{total} remained significantly associated with RFS in multivariable analyses (Table 2A). Furthermore, when similar cox regression univariate and multivariate analysis was performed for CAS_i and CAS_m separately CAS_i and CAS_m was the strongest and most significant independent predictor of RFS respectively (Supplementary Table 3A and 4A) Similar results were evident for the cases that were treated only with lumpectomy (Supplementary Fig. 14).

To verify whether CAS_{total}, CAS_i, and CAS_m could be used to stratify patients in the VC, we used pre-determined CAS cutoffs from the DC (Fig. 3). We found that high CAS_i, CAS_m and CAS_{total} were associated with poorer RFS compared to low CAS_i, CAS_m and CAS_{total}, respectively. Of the patients with LR, 75% were classified into the high CAS_i group (Fig. 3D) and ~67% of patients with LR were classified into the high CAS_{total} subgroups (Fig. 3E). Of the patients in the recurrence-free group, 87% were classified in the low CAS_m group (Fig. 3F). In both univariate and multivariate analyses after adjusting for potentially confounding effects of factors like age, grade, RT and receptor status CAS_{total} and comedo necrosis was the strongest and most significant independent predictor of RFS (i.e., HRs for CAS_{total} were higher than HRs of all other clinicopathologic factors (Table 2B). Similar to DC we observed that CAS_i and CAS_m also independently predicted the RFS (Supplementary Table 3B and 4B).

In addition we performed the bootstrap analysis for the COX regression univariate and multivariate models on the combined (DC+VC=252) dataset and observed that mean HR for the univariate analysis is 5.22 and the multivariate analysis conditional on all other variables is 6.58 ($p < 0.0001$) (Supplementary Fig. 15 and Supplementary Table 5). Also, CAS_{total} was able to identify patients for both DCIS (Supplementary Fig. 16A and B, Supplementary Table 8Ai and 8Bii) and invasive recurrence even after adjusting for potentially confounding effects of factors like age, grade, and RT (Supplementary Fig. 16C and D, Supplementary Table 8AiI and 8Bii) in both DC and VC. (clinicopathological characteristics summarized in Supplementary Table 6 and 7).

Further, in both the DC and VC, the 10-year estimated risk of LR increased continuously as the CAS increased (Supplementary Fig. 17). Next, we determined if our survival model had high predictive accuracy using the Harrell's concordance index. The higher the concordance

index, the better the survival model discriminates between patients who experienced LR versus those who remained LR-free. The results indicated that any patient with a poorer/shorter RFS had a 72.6% probability of being in the high CAS_{total} group. Also, we created a 2×2 confusion matrix performance metrics to show the accuracy of CAS to predict 10-year LR. To do so, we calculated the sensitivity (Sn), specificity (Sp), positive predictive value (PPV), negative predictive value (NPV) and accuracy (Acc) of CAS and odds ratio (OR which represents the increase in odds of a patient in a high-risk group developing recurrence relative to a patient in a low-risk group), for both cohorts to compare the performance of CAS with that of the traditional clinicopathological variables (those used in the Cox regression analysis). As presented in the tables below, our CAS_{total} yielded an accuracy (or Acc) of 0.60, sensitivity of 0.85, specificity of 0.53, PPV of 0.32, NPV of 0.93, and OR of 6.8 in the DC (Supplementary Table 9). We noticed that the CAS_{total} produced a lower accuracy and specificity compared to comedo necrosis (0.71). However, comparison of the Sp, PPV, NPV, and OR performance metrics showed the overall superiority of CAS_{total}, in both cohorts, when compared to the clinicopathologic variables.

Thus, these results collectively show that CAS can robustly predict 10-year LR risk for DCIS patients from two different cohorts.

4. CAS can identify patients who could benefit from radiotherapy

In the DC, CAS_{total} stratified DCIS patients treated with surgery (mastectomy/BCS) or BCS alone (Supplementary Fig. 18B and 18C) into subgroups with high and low LR risks with greater significance relative to patients treated with surgery (mastectomy/BCS) and post-operative RT (Supplementary Fig. 18A) (HR=11.6, p<0.0001 for surgery alone; HR=17.05, p=0.0005 for BCS alone, and HR=2.4, p=0.3589 for surgery + RT). Similarly, in the VC, CAS stratified DCIS patients treated with surgery only (Supplementary Fig 19A and 19B) into subgroups with high and low LR risks with higher significance compared to patients treated with surgery (mastectomy or BCS) and post-operative adjuvant RT (surgery +RT) (HR=3.97, p=0.049 for surgery alone and HR=1.4, p=0.109 for surgery+RT). These data suggest that CAS_{total} can identify LR patients who might benefit from adjuvant RT. In addition, we observed that DCIS patients who recurred as IBC exhibited higher CAS_{total} (p=0.07) compared to the patients who recurred as DCIS (Supplementary Fig. 20) in the DC.

We next evaluated the clinical significance of CAS by examining the associations of CAS with traditionally-employed clinicopathological variables i.e., age, grade, tumor size, comedo necrosis, and RT (Supplementary Figs. 21 and 22). Our data shows that CAS_{total} provides clinically-relevant prognostic information over and beyond what is provided by current clinicopathologic parameters alone. Given that high CA is associated with more aggressive disease phenotypes, we not only observed the association of high CAS_{total} with higher recurrence rates (RR), but also found that CAS_{total} segments patient subgroups more deeply than traditional clinicopathologic parameters (see RR forest plot in Supplementary Fig. 16A). For example, the RR forest plot (Supplementary Fig. 23A) for high grade DCIS patients in the DC showed that patients with comedo necrosis (red), are at high risk of recurrence (0.59) compared to the overall RR for patients (0.33), regardless of the CAS of their tumors. When we further stratified these DCIS patients with comedo necrosis into high

(green) and low (blue) CAS groups, we observed that the RR for the high CAS group (green) was 0.83 and RR for the low CAS subgroup (blue) was 0.10. Similar results were observed for VC (see RR forest plot in Supplementary Fig. 23B). Thus, CAS was able to more deeply segment the patients with comedo necrosis into high and low risk LR groups. Similar trends were evident for tumor size, RT, and age.

5. CAS stratification of DCIS patients into LR and LR-free groups is superior to that afforded by the Van Nuys Prognostic Index (VNPI)

The widely used VNPI is based on patients' age at diagnosis, tumor size, resection margin width and tumor grade. To test the performance of this index in our (DC and VC combined) cohort, we calculated VNPI based on scoring methods described in the literature. Each of the factors was assigned a score between 1–3, and the sum of scores for the four parameters (i.e., the final VNPI score) was used to stratify patients into high, low and intermediate risk groups for LR, employing the binary cutoff score of 8. Next, we compared the performance of VNPI and CAS_{total} in cases from the DC and VC (n=164) (Fig. 4A and 4B) using univariate and Kaplan Meier survival analyses. We found that higher VNPI was not significantly associated with poorer RFS and VNPI did not significantly stratify patients as high and low risk of LR subgroups. By contrast, CAS_{total} stratified DC and VC patients into subgroups of high and low risk of LR with greater significance and HRs (CAS_{total} HR=5.6 vs. VNPI HR=0.70) (Supplementary Table 10). Multivariable analyses adjusted for other potentially confounding factors, such as tumor size, presence of comedo necrosis, age, and RT along with VNPI and CAS, revealed that CAS_{total} showed the highest association with RFS, with a HR=6.86 (Supplementary Table 11). These findings compellingly suggest that the CAS stratification of DCIS patients is superior to that of the traditional VNPI index.

Discussion

DCIS exhibits considerable inter-patient heterogeneity and has a poorly understood natural history. A lack of accurate models for prediction of risk of LR results in over- and under-treatment, complicated by the variable prognostic evidence of patient age, tumor margins, DCIS grade, and size. CA is a hallmark of cancers and is observable in >80% of breast tumors including pre-invasive lesions, and is associated with high grade in DCIS and IBC (18,19). Amplified centrosomes are present in premalignant cells and increase as the disease progresses to dysplasia, highlighting the potential involvement of CA in neoplastic transformation and progression (25).

Our laboratory has previously shown that (a) high levels of CA are associated with poor progression-free survival in invasive breast tumors, and (b) CA is higher in the aggressive TNBC subtype compared to grade-matched non-TNBCs (26,27). This notion was further validated by analysis of the CA20 gene score, which is based on genes associated with CA (28). Recent studies have reported that higher CA induces high-grade features in BCs; thus, CA has been associated with tumor evolution (29). Although studies have reported that BCs exhibit structurally amplified centrosomes, they have not yet established the prognostic value of this structural CA (30). This may be due, in part, to the 2D (i.e., cross-sectional) approaches used in these studies, which have limitations to accurately capture the 3D size of

the centrosome. Moreso, most studies (31) examining CA in BCs have not rigorously evaluated confounding effects of other clinicopathologic variables on the prognostic value of CA.

Our new semi-automated methodology uses quantitative centrosomal phenotyping and an algorithm to measure both numerical and structural centrosomal aberrations in DCIS tumors. For each sample, a continuous CAS was computed that categorized patients as having a high or low 10-year risk of LR. Findings from our retrospective study, which involved two large, well-characterized cohorts (DC and VC) of DCIS cases, showed that patients with LR within 10 years exhibited higher CAS_{total} relative to LR-free patients. Our study is the first to show that organellar-level differences distinguish DCIS patients with LR from LR-free patients, and that high levels of both numerical and structural CA are associated with increased 10-year risk of LR in DCIS patients. Our results suggest that aberrant centrosomal homeostasis in DCIS drives pathophysiological alterations that potentially facilitate disease progression through CIN-dependent as well as CIN-independent mechanisms. While CA may drive ITH through CIN, an increased centrosome complement may, via modulation of the microtubule cytoskeleton, enhance directional migration and invasion of malignant cells and thus enhance the risk of LR in the longer term (32). We have demonstrated that CAS_{total} is significantly and independently associated with poor RFS, and upon inclusion of both CAS_{total} and VNPI into multivariable models, we found that CAS_{total} outperforms VNPI in predicting LR. CAS_{total} predicts the 10-year risk of LR with higher concordance than VNPI. In DCIS patient subsets, defined based on their clinical and histopathological parameters, stratification by CAS_{total} prognostically augmented several clinicopathologic parameters in determining rate of recurrence. Among subsets of DCIS patients treated with BCS or those receiving additional adjuvant RT, CAS_{total} identified patients with high risk of LR. Thus, CAS_{total} can be used as a clinical tool to identify patients who can be safely treated with BCS/mastectomy alone, and those who will benefit from the inclusion of RT. Our centrosomal profiling methodology, which dichotomizes DCIS patients into high- and low- risk categories, enables clear go/no-go therapeutic decision making, and can substantially augment individualized management of DCIS based upon risk conferred by the patient's centrosomal complement.

CAS, as the linear expression of the severity and frequency of numerical and structural CA, may serve as an indirect measure of ITH in DCIS. Our study, the first to robustly quantify CA in both pure and mixed DCIS samples, has contributed evidence supporting a model of CA-driven DCIS progression into IBC. These findings concur with previous studies wherein we, and others, observed that TNBC, the most aggressive subtype of BC, exhibits highest CA among all BC subtypes (26,29). Centrosome profiling can complement clinicopathologic and genomic evaluation to provide a comprehensive portrait of disease status. An exciting avenue for future research is to profile CA in all the stages of tumor progression starting from atypical hyperplasia to invasive and metastatic disease to evaluate if CA can function as a biomarker for tumor evolution.

The commercially available Oncotype Dx DCIS score is applicable mainly to cases with resection margins of at least 3 mm and low/intermediate-grade DCIS measuring ≥ 2.5 cm, or in high-grade DCIS of ≥ 1 cm, as this is the set of patients from the ECOG 5194 study upon

which the test was initially clinically validated (11). By contrast, our quantitative centrosomal phenotyping methodology is more broadly applicable and could be refined for other cancer types with rampant CA. The gene signature that comprises the basis of the Oncotype DCIS Score consists mainly of proliferation-related genes. CA is a phenotypic biomarker that serves as a readout of hundreds of deregulated signaling pathways that culminate in numerical and/or structural CA, including dysregulated proliferation-related signaling cascades. Thus, our methodology captures prognostic information from a broader swath of biological pathways that are deregulated in and drive the biology of DCIS. CAS-based risk profiling of core biopsies may reduce the number of re-excisions even in the event of close/positive margins.

However, our study has a few limitations. There are imbalances in the number of patients in different subgroups, in the DC and the VC of the study, which has resulted in better performance of CAS (higher HR) in the DC. While the DC has more high-grade patients, the VC has a balanced number of high, intermediate, and low-grade patients. High-grade patients tend to present with invasive recurrence. A higher number of patients recurred as invasive in the DC and patients with invasive recurrence exhibited higher CAS when compared to patients who recurred as DCIS in DC. Whereas, in VC due to more balanced numbers of high, intermediate, and low-grade patients, no such variation in the type of LR was observed. Furthermore, lack of receptor status in some cases precluded study of the confounding effect of receptors in this dataset. The study cohort did not include any patients treated with endocrine therapy. These limitations in the DC and VC perhaps lead to the slightly different performance of CAS among the two cohorts. Validation studies in external cohorts and mechanistic studies to understand the role of CA-associated proteins in DCIS progression model are warranted.

Supplementary Material

Refer to Web version on PubMed Central for supplementary material.

Acknowledgments:

This study was supported by grants to RA from the National Cancer Institutes of Health (U01 CA179671) and a graduate fellowship to KM from the Second Century Initiative Program at Georgia State University.

References

1. Silverstein MJ, Lagios MD, Recht A, Allred DC, Harms SE, Holland R, et al. Image-detected breast cancer: state of the art diagnosis and treatment. *J Am Coll Surg* 2005;201(4):586–97 doi 10.1016/j.jamcollsurg.2005.05.032. [PubMed: 16183499]
2. Independent UKPoBCS. The benefits and harms of breast cancer screening: an independent review. *Lancet* 2012;380(9855):1778–86 doi 10.1016/S0140-6736(12)61611-0. [PubMed: 23117178]
3. Page DL, Dupont WD, Rogers LW, Landenberger M. Intraductal carcinoma of the breast: follow-up after biopsy only. *Cancer* 1982;49(4):751–8. [PubMed: 6275978]
4. Esserman L, Yau C. Rethinking the Standard for Ductal Carcinoma In Situ Treatment. *JAMA Oncol* 2015;1(7):881–3 doi 10.1001/jamaoncol.2015.2607. [PubMed: 26291410]
5. Benson JR, Wishart GC. Predictors of recurrence for ductal carcinoma in situ after breast-conserving surgery. *Lancet Oncol* 2013;14(9):e348–57 doi 10.1016/S1470-2045(13)70135-9. [PubMed: 23896274]

6. Freedman GM, Fowble BL. Local recurrence after mastectomy or breast-conserving surgery and radiation. *Oncology (Williston Park)* 2000;14(11):1561–81; discussion 81–2, 82–4. [PubMed: 11125941]
7. Silverstein MJ, Lagios MD. Treatment selection for patients with ductal carcinoma in situ (DCIS) of the breast using the University of Southern California/Van Nuys (USC/VNPI) prognostic index. *Breast J* 2015;21(2):127–32 doi 10.1111/tbj.12368. [PubMed: 25600630]
8. Rudloff U, Jacks LM, Goldberg JI, Wynveen CA, Brogi E, Patil S, et al. Nomogram for predicting the risk of local recurrence after breast-conserving surgery for ductal carcinoma in situ. *J Clin Oncol* 2010;28(23):3762–9 doi 10.1200/JCO.2009.26.8847. [PubMed: 20625132]
9. Boland GP, Chan KC, Knox WF, Roberts SA, Bundred NJ. Value of the Van Nuys Prognostic Index in prediction of recurrence of ductal carcinoma in situ after breast-conserving surgery. *Br J Surg* 2003;90(4):426–32 doi 10.1002/bjs.4051. [PubMed: 12673743]
10. Momtahn S, Curtin J, Mittal K. Current Chemotherapy and Potential New Targets in Uterine Leiomyosarcoma. *J Clin Med Res* 2016;8(3):181–9 doi 10.14740/jocmr2419w. [PubMed: 26858789]
11. Solin LJ, Gray R, Baehner FL, Butler SM, Hughes LL, Yoshizawa C, et al. A multigene expression assay to predict local recurrence risk for ductal carcinoma in situ of the breast. *J Natl Cancer Inst* 2013;105(10):701–10 doi 10.1093/jnci/djt067. [PubMed: 23641039]
12. Casasent AK, Schalck A, Gao R, Sei E, Long A, Pangburn W, et al. Multiclonal Invasion in Breast Tumors Identified by Topographic Single Cell Sequencing. *Cell* 2018;172(1–2):205–17 e12 doi 10.1016/j.cell.2017.12.007. [PubMed: 29307488]
13. Miron A, Varadi M, Carrasco D, Li H, Luongo L, Kim HJ, et al. PIK3CA mutations in in situ and invasive breast carcinomas. *Cancer Res* 2010;70(14):5674–8 doi 10.1158/0008-5472.CAN-08-2660. [PubMed: 20551053]
14. Yap TA, Gerlinger M, Futreal PA, Pusztai L, Swanton C. Intratumor heterogeneity: seeing the wood for the trees. *Sci Transl Med* 2012;4(127):127ps10 doi 10.1126/scitranslmed.3003854.
15. Godinho SA, Pellman D. Causes and consequences of centrosome abnormalities in cancer. *Philos Trans R Soc Lond B Biol Sci* 2014;369(1650) doi 10.1098/rstb.2013.0467.
16. McBride M, Rida PC, Aneja R. Turning the headlights on novel cancer biomarkers: Inspection of mechanics underlying intratumor heterogeneity. *Mol Aspects Med* 2015;45:3–13 doi 10.1016/j.mam.2015.05.001. [PubMed: 26024970]
17. Nigg EA. Centrosome duplication: of rules and licenses. *Trends Cell Biol* 2007;17(5):215–21 doi 10.1016/j.tcb.2007.03.003. [PubMed: 17383880]
18. Chan JY. A clinical overview of centrosome amplification in human cancers. *Int J Biol Sci* 2011;7(8):1122–44. [PubMed: 22043171]
19. D'Assoro AB, Lingle WL, Salisbury JL. Centrosome amplification and the development of cancer. *Oncogene* 2002;21(40):6146–53 doi 10.1038/sj.onc.1205772. [PubMed: 12214243]
20. Fukasawa K. Centrosome amplification, chromosome instability and cancer development. *Cancer letters* 2005;230(1):6–19 doi 10.1016/j.canlet.2004.12.028. [PubMed: 16253756]
21. Hoque A, Carter J, Xia W, Hung MC, Sahin AA, Sen S, et al. Loss of aurora A/STK15/BTAK overexpression correlates with transition of in situ to invasive ductal carcinoma of the breast. *Cancer Epidemiol Biomarkers Prev* 2003;12(12):1518–22. [PubMed: 14693746]
22. Toss MS, Miligy IM, Gorringer KL, AlKawaz A, Khout H, Ellis IO, et al. Prolyl-4-hydroxylase Alpha subunit 2 (P4HA2) expression is a predictor of poor outcome in breast ductal carcinoma in situ (DCIS). *Br J Cancer* 2018;119(12):1518–26 doi 10.1038/s41416-018-0337-x. [PubMed: 30410060]
23. Toss MS, Miligy I, Al-Kawaz A, Alsleem M, Khout H, Rida PC, et al. Prognostic significance of tumor-infiltrating lymphocytes in ductal carcinoma in situ of the breast. *Mod Pathol* 2018;31(8):1226–36 doi 10.1038/s41379-018-0040-8. [PubMed: 29559742]
24. Miligy IM, Gorringer KL, Toss MS, Al-Kawaz AA, Simpson P, Diez-Rodriguez M, et al. Thioredoxin-interacting protein is an independent risk stratifier for breast ductal carcinoma in situ. *Mod Pathol* 2018;31(12):1807–15 doi 10.1038/s41379-018-0086-7. [PubMed: 29955142]

25. Lopes CAM, Mesquita M, Cunha AI, Cardoso J, Carapeta S, Laranjeira C, et al. Centrosome amplification arises before neoplasia and increases upon p53 loss in tumorigenesis. *J Cell Biol* 2018;217(7):2353–63 doi 10.1083/jcb.201711191. [PubMed: 29739803]
26. Pannu V, Mittal K, Cantuaria G, Reid MD, Li X, Donthamsetty S, et al. Rampant centrosome amplification underlies more aggressive disease course of triple negative breast cancers. *Oncotarget* 2015;6(12):10487–97 doi 10.18632/oncotarget.3402. [PubMed: 25868856]
27. Mittal K, Choi DH, Ogden A, Donthamsetty S, Melton BD, Gupta MV, et al. Amplified centrosomes and mitotic index display poor concordance between patient tumors and cultured cancer cells. *Sci Rep* 2017;7:43984 doi 10.1038/srep43984. [PubMed: 28272508]
28. Ogden A, Rida PC, Aneja R. Prognostic value of CA20, a score based on centrosome amplification-associated genes, in breast tumors. *Sci Rep* 2017;7(1):262 doi 10.1038/s41598-017-00363-w. [PubMed: 28325915]
29. Denu RA, Zasadil LM, Kanugh C, Laffin J, Weaver BA, Burkard ME. Centrosome amplification induces high grade features and is prognostic of worse outcomes in breast cancer. *BMC Cancer* 2016;16:47 doi 10.1186/s12885-016-2083-x. [PubMed: 26832928]
30. Guo HQ, Gao M, Ma J, Xiao T, Zhao LL, Gao Y, et al. Analysis of the cellular centrosome in fine-needle aspirations of the breast. *Breast Cancer Res* 2007;9(4):R48 doi 10.1186/bcr1752. [PubMed: 17662154]
31. D'Assoro AB, Barrett SL, Folk C, Negron VC, Boeneman K, Busby R, et al. Amplified centrosomes in breast cancer: a potential indicator of tumor aggressiveness. *Breast Cancer Res Treat* 2002;75(1):25–34. [PubMed: 12500932]
32. Ogden A, Rida PC, Aneja R. Heading off with the herd: how cancer cells might maneuver supernumerary centrosomes for directional migration. *Cancer Metastasis Rev* 2013;32(1–2):269–87 doi 10.1007/s10555-012-9413-5. [PubMed: 23114845]

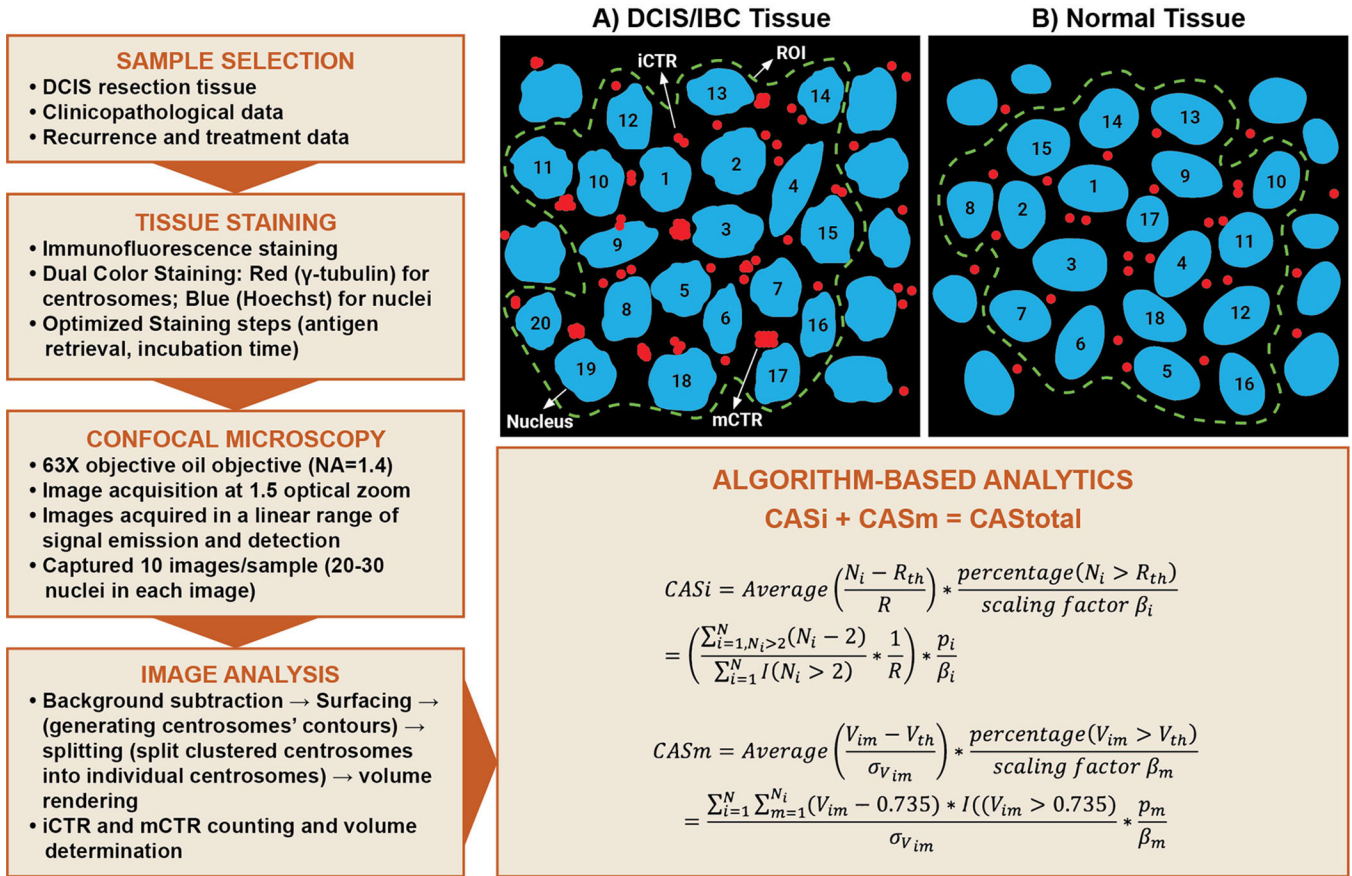


Figure 1.

Schematic depicting semi-automated workflow to quantify CA in clinical samples. A description of terms used in the algorithm is provided in the Methods section. **(A)** Centrosomes in breast tissues (normal, DCIS or IBC) were categorized into individually distinguishable centrosomes (iCTRs) and megacentrosomes (mCTRs). iCTRs were defined as centrosomes that stain positive for γ -tubulin and whose volumes lie within the range of centrosome volumes found in normal breast tissue stained for γ -tubulin. **(B)** mCTRs were defined as centrosomes in a neoplastic region that stain positive for γ -tubulin and whose volume is greater than the upper limit of the centrosome volume range found in corresponding normal tissue immunostained for γ -tubulin. Thus, mCTRs are centrosomes with aberrantly large volumes and are considered to represent structurally amplified centrosomes.

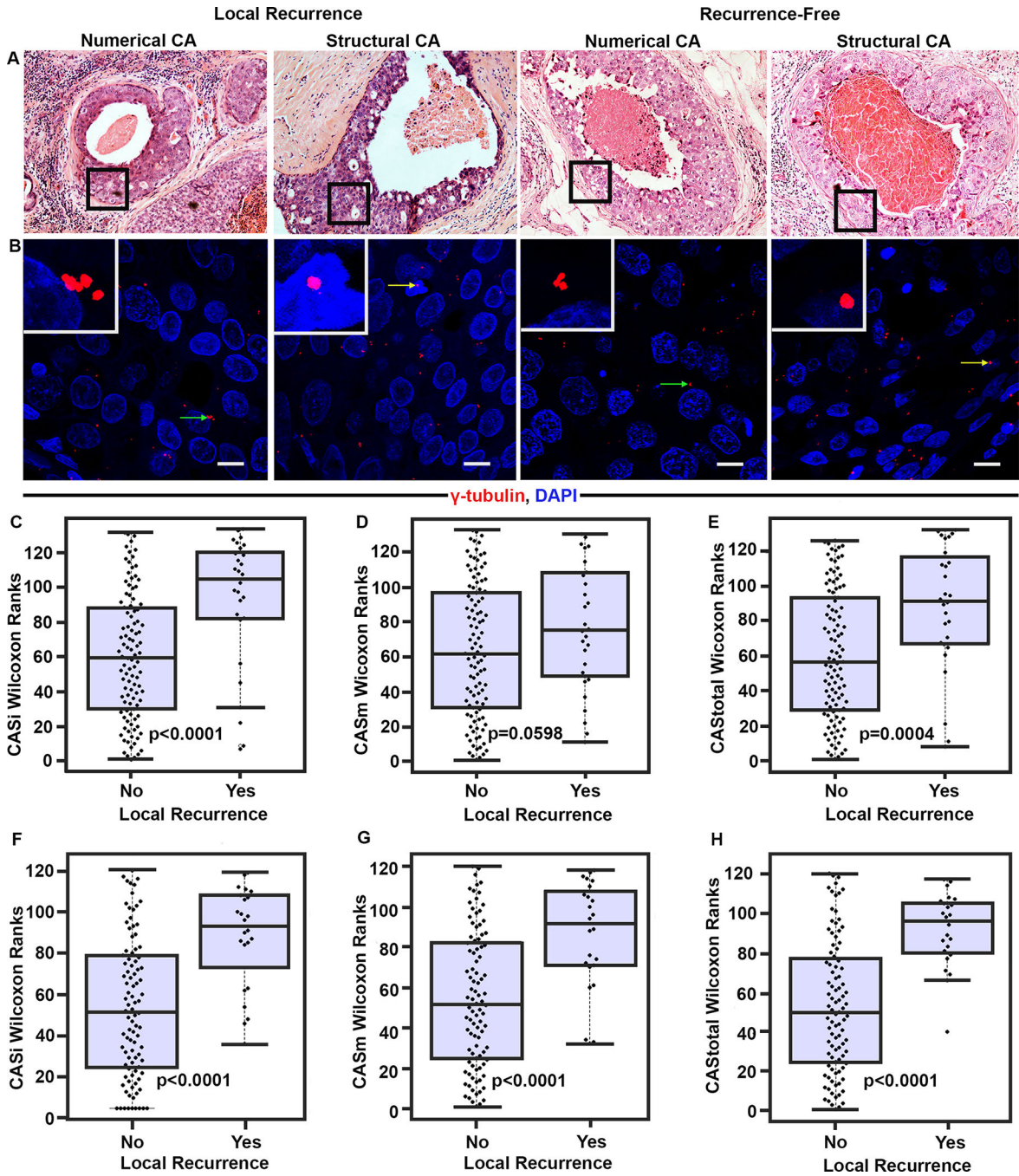


Figure 2: DCIS cases in the DC with ipsilateral recurrence exhibit higher CAS than recurrence-free cases. (A) Representative H&E images (20 \times magnification) of the ducts from DCIS cases with and without LR. Black boxes represent the area magnified in panel B. (B) Confocal micrographs showing numerical (green arrows) and structural (yellow arrows) CA in DCIS with or without recurrence. Tissue sections were immunostained for centrosomes (γ -tubulin, red) and nuclei (Hoechst, blue). Scale bar (white), 20 μ m. Beeswarm box plots showing Wilcoxon ranks for pure DCIS cases with LR (n=28) and without LR (n=105). (C) CASi (D)

CASm (**E**) CASTotal. $p < 0.05$ was considered statistically significant. Beeswarm box plots showing Wilcoxon ranks for pure DCIS cases with LR (n=24) and LR-free cases (n=95) in VC (**F**) CASi, (**G**) CASm, and (**H**) CASTotal. $p < 0.05$ was considered statistically significant.

Author Manuscript

Author Manuscript

Author Manuscript

Author Manuscript

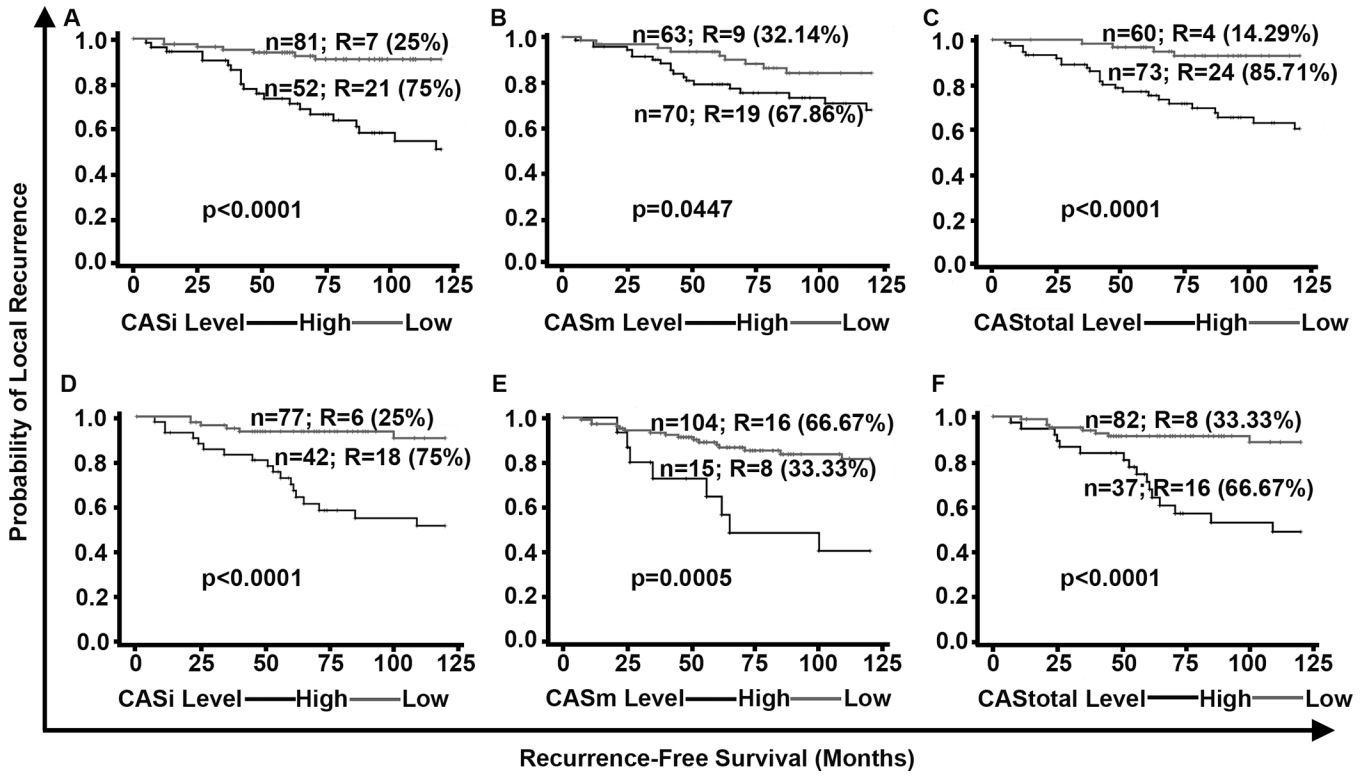


Figure 3:

In the DC and VC, higher CAS is associated with poorer RFS. Kaplan Meier survival curves representing the RFS of patients in the DC stratified into (A) CASi high and low groups, (B) CASm high and low groups, (C) CASTotal high and low groups. Kaplan Meier curves representing the RFS of DCIS patients in the VC stratified into (D) CASi high and low groups, (E) CASm high and low groups, and (F) CASTotal high and low groups. N: total number of patients in each group; R: number of patients who developed LR; % represents the percentage/proportion of patients with LR out of the total number of patients with LR in both groups combined.

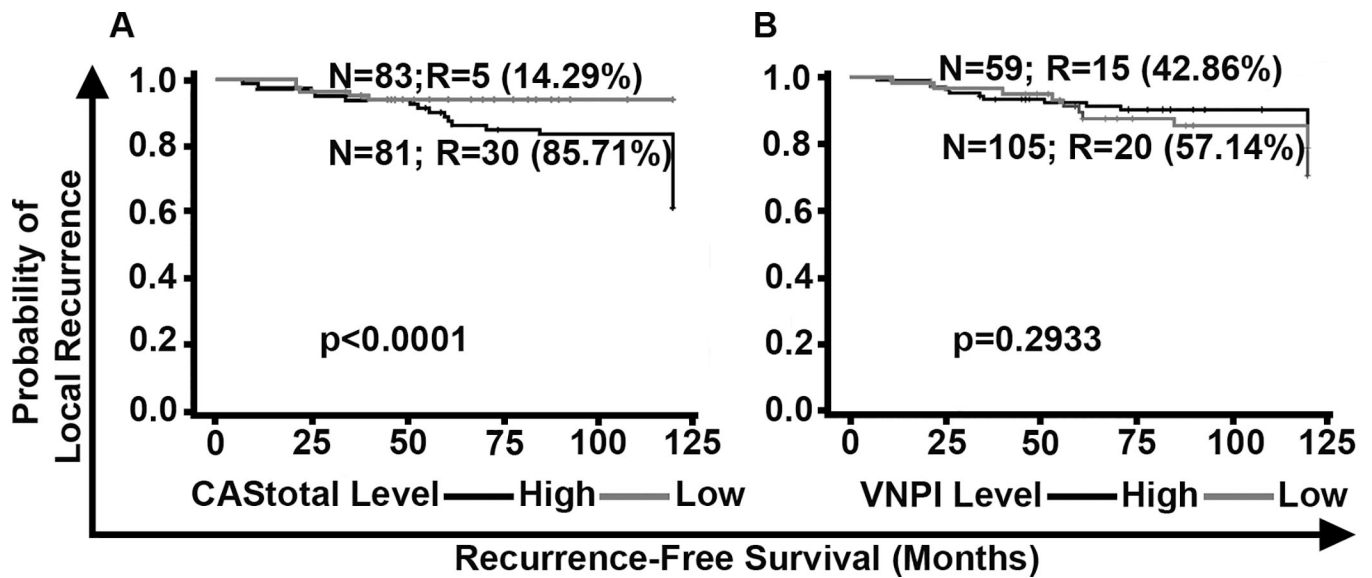


Figure 4:
 Comparison of the stratification of DCIS patients by CAStotal and Van Nuys Prognostic Index (VNPI). Kaplan Meier survival curves representing the RFS of DCIS patients (n=164) stratified by (A) CAStotal, and (B) VNPI. N: total number of patients in each group; R: number of patients who showed LR; %: percentage/proportion of patients with LR out of the total number of patients with LR in the DC and VC combined.

Table 1:

Descriptive statistics of clinicopathological characteristics for pure DCIS based on the recurrence status in the (A) DC and (B) VC. The χ^2 p-values were used to determine if the differences in proportions were statistically significant.

A			
Discovery Cohort Overall Clinical Characteristics			
Baseline Characteristics	Recurrence-Free	Local Recurrence	p-value
Patient Age, n(%)			
Age>50	87 (82.86)	22 (78.57)	0.6003
Age<=50	18 (17.14)	6 (21.43)	
Tumor Size, n(%)			
Size>16	51 (48.57)	15 (53.57)	0.6382
Size<=16	54 (51.43)	13 (46.43)	
Grade, n(%)			
High	97 (92.38)	21 (75.00)	0.0098
Mid and Low	8 (7.62)	7 (25.00)	
Comedo Necrosis, n(%)			
No	14 (13.33)	8 (28.57)	0.0538
Yes	91 (86.67)	20 (71.43)	
Radiotherapy, n(%)			
No	57 (54.29)	21 (75.00)	0.0480
Yes	48 (45.71)	7 (25.00)	
Receptor Status, n(%)			
ER/PR/HER2-Positive	3 (2.86)	2 (7.14)	0.6826
ER/PR-Positive and HER2-Negative	20 (19.05)	7 (25.00)	
HER2-Positive	8 (7.62)	2 (7.14)	
TNBC	9 (8.57)	1 (3.57)	
Missing	65 (61.90)	16 (57.14)	
B			
Validation Cohort Overall Clinical Characteristics			
Baseline Characteristics	Recurrence-Free	Local Recurrence	p-value
Patient Age, n(%)			
Age>50	68 (71.58)	12 (50.00)	0.0442
Age<=50	27 (28.42)	12 (50.00)	
Tumor Size, n(%)			
Size>16	81 (85.26)	9 (37.50)	<0.0001
Size<=16	14 (14.74)	15 (62.50)	
Grade, n(%)			
High	47 (49.47)	12 (50.00)	0.9632

B			
Validation Cohort Overall Clinical Characteristics			
Baseline Characteristics	Recurrence-Free	Local Recurrence	p-value
Mid and Low	48 (50.53)	12 (50.00)	
Comedo Necrosis, n(%)			
No	37 (38.95)	16 (66.67)	0.0146
Yes	58 (61.05)	8 (33.33)	
Radiotherapy, n(%)			
No	83 (87.37)	22 (91.67)	0.5593
Yes	12 (12.63)	2 (8.33)	
Receptor Status, n(%)			
ER/PR/HER2-Positive	9 (9.78)	4 (14.81)	0.4706
ER/PR-Positive and HER2-Negative	37 (40.22)	15 (55.56)	
HER2-Positive	13 (14.13)	2 (7.41)	
TNBC	6 (6.52)	1 (3.70)	
Missing	27 (29.35)	5 (18.52)	

Author Manuscript

Author Manuscript

Author Manuscript

Author Manuscript

Table 2:

Univariate and multivariate Cox proportional regression analysis for the risk of LR in DCIS treated with BCS or mastectomy comparing the influence of common clinicopathological variables relative to CAStotal in (A) DC and (B) VC.

A									
Discovery Cohort Cox Regression									
Variables		Univariate Analysis				Multivariate Analysis			
		p-value	Hazard Ratio	95% Hazard Ratio Confidence Limits		p-value	Hazard Ratio	95% Hazard Ratio Confidence Limits	
Recurrence-Free Survival									
CAStotal	High vs Low	<0.001	6.337	2.196	18.287	<0.001	7.869	2.709	22.857
Age	>50 years vs <=50 years	0.437	0.697	0.280	1.733	0.599	0.767	0.284	2.068
Grade	High vs intermediate/low	0.009	0.317	0.134	0.752	0.022	0.257	0.081	0.823
Comedo Necrosis	Present vs absent	0.088	2.043	0.899	4.640	0.271	1.635	0.681	3.926
Radiotherapy	No vs yes	0.128	1.946	0.826	4.583	0.403	1.470	0.596	3.628
Receptor status	ER/PR positive HER2 negative	0.194	1.719	0.759	3.893	0.163	2.044	0.748	5.581
	ER/PR/HER2 negative	0.663	0.638	0.084	4.821	0.977	0.969	0.120	7.835
	ER/PR/HER2 positive	0.240	2.425	0.553	10.640	0.323	2.329	0.435	12.456
	HER2 positive	0.534	1.480	0.430	5.089	0.214	2.458	0.595	10.151

B									
Validation Cohort Cox Regression									
Variables		Univariate Analysis				Multivariate Analysis			
		p-value	Hazard Ratio	95% Hazard Ratio Confidence Limits		p-value	Hazard Ratio	95% Hazard Ratio Confidence Limits	
Recurrence-Free Survival									
CAStotal	High vs Low	<0.001	4.820	2.041	11.384	<0.001	5.569	2.310	13.427
Age	>50 years vs <=50 years	0.154	0.535	0.227	1.263	0.011	0.328	0.138	0.776
Grade	High vs intermediate/low	0.954	0.976	0.430	2.216	0.461	1.404	0.569	3.464
Comedo Necrosis	Present vs absent	0.026	2.652	1.123	6.259	0.008	5.817	1.590	21.283
Radiotherapy	No vs yes	0.853	1.148	0.268	4.916	0.923	0.925	0.191	4.483
Receptor status	ER/PR positive HER2 negative	0.312	1.686	0.612	4.646	0.330	0.518	0.138	1.947
	ER/PR/HER2 negative	0.881	0.848	0.099	7.275	0.347	3.018	0.302	30.159
	ER/PR/HER2 positive	0.286	2.047	0.549	7.641	0.913	0.921	0.212	4.006
	HER2 positive	0.667	0.697	0.135	3.608	0.664	1.464	0.262	8.171